

Figure 1. Steady-state fluorescence spectra of 1-4 in pentane excited at 310 nm. The spectrum of 4 contains a noticeable contribution from the 5,6-di-*p*-tolyl-2,9-dimethylphenanthrene cyclization product in the wavelength range 340-440 nm.

It contains emission from S_{IV} and from S_{IR} prior to the attainment of equilibrium with $^1p^*$. The slow component makes up most of the fluorescence decay at 650 nm. The fluorescence decay from 4 is analogous to that from 1, with a slow decay rate constant of $8 \times 10^8 \text{ s}^{-1}$.

For 2 in MCH, the fluorescence decay follows the system response at all wavelengths. Experiments with faster time resolution are needed to compare the S_{IR} and $^1p^*$ lifetimes in 2. However, the kinetic model in Scheme I should explain the difference in fluorescence quantum yields for 1 and 2, provided all of the rate constants can be estimated (Scheme I). The radiative rate constant, k_r , is obtained from ref 4d. The inverse of the $^1p^*$ appearance time constant^{4a} is used as an estimate of k_2 , and the $^1p^*$ decay rate constant is approximated by the entries in column 4 of Table I. k_{-2} is obtained from $RT \ln(k_2/k_{-2}) = |\Delta G^\circ|$, where the free energy difference between S_{IR} and $^1p^*$, $|\Delta G^\circ|$, is estimated as 2.5 kcal/mol. For 1, Φ_f and Φ_s , the fluorescence quantum yields of the fast and slow S_{IR} decays, are predicted to be 0.001 and 0.005, respectively. If $|\Delta G^\circ|$ is 1 kcal/mol larger for 2, Φ_f and Φ_s are 0.001 and 0.0003, respectively. These estimates qualitatively reproduce the observed trend in the quantum yields, without assuming any change in the $S_{IR} \rightarrow ^1p^*$ barrier. The explanation for the quantum yield changes based on a decrease in the $S_{IR} \rightarrow ^1p^*$ barrier cannot explain the nonexponential S_{IR} fluorescence decays.

Interconversion of vertical and twisted arylalkene excited states has been detected in other systems. Equilibration in the triplet manifold for stilbenes and tri- and tetraphenylethylene⁹ is well documented, and recently, Saltiel observed a very low quantum yield for emission from excited *trans*-stilbene following excitation of the *cis* isomer.¹⁰ The low quantum efficiency of this process in stilbenes is due, in part, to the ultrashort lifetime of the intervening twisted state. In 1, 3, and 4, the long $^1p^*$ lifetime and small $S_{IR} \rightarrow ^1p^*$ energy gap (<10 kcal/mol) permit thermal repopulation of and a significant delayed fluorescence quantum yield from S_{IR} . The decreased lifetime and energy of the zwitterionic $^1p^*$ state in 2 significantly reduce the repopulation of S_{IR} and its fluorescence quantum yield.¹¹ Studies to determine the $^1p^*$ energy

in 2 and the solvent- and temperature-dependent quantum yields¹⁴ and lifetimes from S_{IR} in 1-4 are currently in progress.

Acknowledgment is made to the donors of the Petroleum Research Fund, administered by the American Chemical Society, for partial support of this research. Financial support from the 3M Corporation and from an NSF Presidential Young Investigator Award to M.B.Z. is gratefully acknowledged. We thank Professor E. Hilinski for numerous discussions and Professor J. Saltiel for repeatedly asking why no excited-state equilibrium was present in TPE.

(12) (a) Nebot-Gil, I.; Malrieu, J.-P. *J. Am. Chem. Soc.* **1982**, *104*, 3320. (b) Malrieu, J.-P.; Nebot-Gil, I.; Sanchez-Marín, J. *Pure Appl. Chem.* **1984**, *56*, 1241.

(13) (a) Bromberg, A.; Schmidt, K. H.; Meisel, D. *J. Am. Chem. Soc.* **1984**, *106*, 3056. (b) Meisel, D.; Das, P. K.; Hug, G. L.; Bhattacharyya, K.; Fessenden, R. W. *J. Am. Chem. Soc.* **1986**, *108*, 4706. (c) Bromberg, A.; Meisel, D. *J. Phys. Chem.* **1985**, *89*, 2507.

(14) The temperature and viscosity dependences of the complete TPE fluorescence spectrum have been analyzed previously. (a) Stegemeyer, H. *Ber. Bunsenges. Phys. Chem.* **1968**, *72*, 335. (b) Sharafy, S.; Muszkat, K. A. *J. Am. Chem. Soc.* **1971**, *93*, 4119.

A Stable Carbene-Alane Adduct

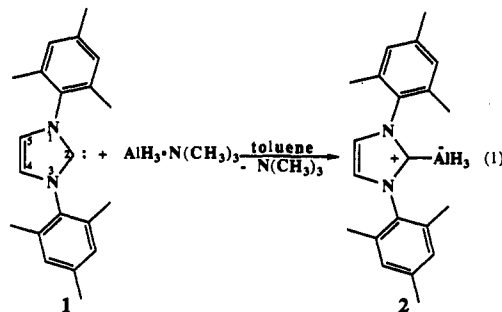
Anthony J. Arduengo, III,* H. V. Rasika Dias,
Joseph C. Calabrese, and Fredric Davidson

Contribution No. 6314, Du Pont Central Research
Experimental Station
Wilmington, Delaware 19880-0328

Received September 11, 1992

There are no reports of main group III adducts of carbenes. Herein, we report a high-yield synthesis and characterization of a stable compound of this type, 1,3-bis(2,4,6-trimethylphenyl)imidazol-2-ylidene- AlH_3 (2).

Compound 2 was obtained in quantitative yield by treatment of 1,3-bis(2,4,6-trimethylphenyl)imidazol-2-ylidene (1)¹ with $\text{Me}_3\text{N}\cdot\text{AlH}_3$ ² in toluene.³ Alane adduct 2 is a white solid melting at 246-247 °C. The ¹H NMR spectrum of 2 (THF-*d*₆) shows a resonance for the C_{4,5} imidazole ring protons at δ 7.42. This is shifted downfield from the corresponding resonance in 1 (δ 7.02).¹ The ¹³C NMR signal for C₂ of 2 appears at δ 175.3, substantially upfield from the free carbene (δ 219.7).¹ The ²⁷Al NMR resonance of δ 107 for 2 is typical of 4-coordinate aluminum species.⁴ These resonances suggest an electronic structure for the imidazole fragment which is intermediate between the free carbene and the fully delocalized imidazolium ion (e.g., 3).⁵



(1) Arduengo, A. J., III; Dias, H. V. R.; Harlow, R. L.; Kline, M. *J. Am. Chem. Soc.* **1992**, *114*, 5530.

(2) $\text{AlH}_3\cdot\text{NMe}_3$ was prepared from $\text{Me}_3\text{N}\cdot\text{HCl}$ and LiAlH_4 as previously described. See: Ruff, J. K.; Hawthorne, M. F. *J. Am. Chem. Soc.* **1960**, *82*, 2141; Method A.

(9) (a) Gorner, H. *J. Phys. Chem.* **1982**, *86*, 2028. (b) Gorner, H.; Schulte-Frohlinde, D. *J. Phys. Chem.* **1981**, *85*, 1835.

(10) Saltiel, J.; Waller, A.; Sun, Y.-P.; Sears, D. F., Jr. *J. Am. Chem. Soc.* **1990**, *112*, 4580.

(11) As an alternative explanation, the red emission could derive from an equilibrium between the $^1p^*$ state and the twisted, excited diradical state.¹² Although the diphenylmethyl radical's fluorescence is centered at 540 nm, the spectrum is structured and significantly narrower than the red emission from TPE.¹³ Furthermore, the red emission is seen under conditions where the twisted state is not formed.^{4b} Also, the excited diradical state's energy, 89 kcal/mol, obtained from the twisted ground-state energy⁶ and the diphenylmethyl radical fluorescence maximum,¹³ precludes thermal population of this state from $^1p^*$.

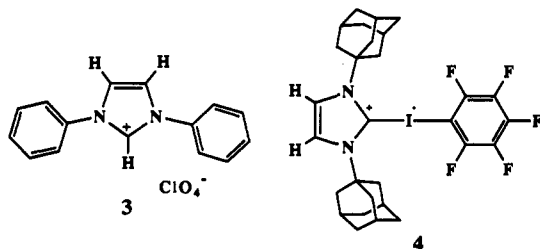
Table I. Selected Bond Lengths (pm) and Angles (deg) in 1-3^a

property	1	2	3 ^{5c}
$r(\text{C}_2\text{-N}_{1(3)})$	136.5 (4), 137.1 (4)	135.5 (3), 135.0 (3)	133.6
$r(\text{C}_4\text{-C}_5)$	133.1 (5)	131.3 (4)	133.9
$r(\text{N}_{1(3)}\text{-C}_{5(4)})$	138.1 (4), 137.8 (4)	138.2 (4), 138.4 (4)	138.0
$r(\text{N}_{1(3)}\text{-mesityl})$	144.1 (4), 144.2 (4)	143.6 (3), 144.2 (3)	143.2 (phenyl)
$r(\text{C}_2\text{-Al})$		203.4 (3)	
$\theta(\text{N}_1\text{-C}_2\text{-N}_3)$	101.4 (2)	104.2 (2)	109.2
$\theta(\text{C}_{5(4)}\text{-N}_{1(3)}\text{-C}_2)$	112.8 (3), 112.8 (3)	110.5 (3), 110.8 (3)	108.0
$\theta(\text{N}_{1(3)}\text{-C}_{5(4)}\text{-C}_{4(5)})$	106.5 (3), 106.5 (3)	107.5 (3), 107.0 (3)	106.5
$\theta(\text{C}_2\text{-N}_{1(3)}\text{-mesityl})$	121.8 (2), 122.6 (2)	124.2 (2), 124.5 (2)	126.6 (phenyl)

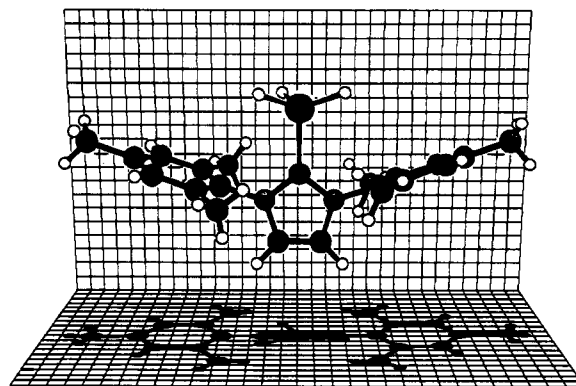
^aThe numbering scheme for all compounds is as indicated for 1.

X-ray quality colorless crystals of **2** were obtained from a THF/toluene solution at -25°C .⁶ The X-ray crystal structure is illustrated with the KANVAS⁷ drawing in Figure 1. Selected bond lengths and angles are given in Table I.

The $\text{C}_2\text{-Al}$ distance is 203.4 (3) pm, which is slightly longer than the Al-C (terminal) distance of 195.8 pm observed for $(\text{AlPh}_3)_2$.⁸ The geometry around C_2 is planar with an average $\text{N}_{1(3)}\text{-C}_2\text{-Al}$ angle of 127.9° and an $\text{N}_1\text{-C}_2\text{-N}_3$ angle of $104.2(2)^\circ$. The $\text{C}_2\text{-N}_{1(3)}$ bond distances (Table I) are intermediate between those in the free carbene and in representative 1,3-diarylimidazolium ions (3).^{5c} The two mesityl groups in **2** are nearly perpendicular to the imidazole ring with twist angles of 82° and 85° .



The intermediate ring geometry, which is reflected in both the angles and bond lengths of **2**, is similar to the geometry observed for a nucleophilic carbene-derivative reverse iodine ylide **4**.⁹ It is remarkable that the ring internal angle at C_2 of **4** was 104.1° (very

Figure 1. KANVAS⁷ drawing of **2**.

close to the same angle in **2**) even though the substituents at N_1 , N_3 , and C_2 are very different. The generality and significance of this type of intermediate imidazole ring geometry are under study.

Structurally well characterized alane adducts are rare,¹⁰ and their carbene complexes are unknown. Compound **2** represents the first example of a main group III-carbene complex and an interesting example of a well-characterized monomeric alane adduct. The stability of **2** is remarkable, considering the fact that it contains a potential hydride donor adjacent to an electrophilic carbon center.

Acknowledgment is made for the excellent technical assistance of H. A. Craig and W. F. Marshall.

Supplementary Material Available: Complete description of the X-ray crystallographic determination on **2**, including tables of fractional coordinates, isotropic and anisotropic thermal parameters, bond distances, and bond angles and ORTEP drawings (10 pages). Ordering information is given on any current masthead page.

(9) Arduengo, A. J., III; Kline, M.; Calabrese, J. C.; Davidson, F. J. *Am. Chem. Soc.* **1991**, *113*, 9704.

(10) (a) Lobkovskii, E. B.; Semenenko, K. N. *Zh. Strukt. Khim.* **1975**, *16*, 150. (b) Atwood, J. L.; Bennett, F. R.; Elms, F. M.; Jones, C.; Raston, C. L.; Robinson, K. D. *J. Am. Chem. Soc.* **1991**, *113*, 8183.

(3) Solid **1** (0.201 g, 0.66 mmol) was added as a single portion to a solution of $\text{AlH}_3\cdot\text{NMe}_3$ (0.059 g, 0.66 mmol) in toluene (30 mL) at room temperature under a dry nitrogen atmosphere. The mixture was stirred for 2 h. Volatiles were removed under vacuum to afford a white residue (0.22 g, 100%): mp $246\text{--}247^\circ\text{C}$; $^1\text{H NMR}$ ($\text{THF-}d_6$) δ 2.06 (s, 12 H, *o*- CH_3), 2.32 (s, 6 H, *p*- CH_3), 2.7 (br s, 3 H, AlH_3), 6.98 (s, 4 H, *m*-H), 7.42 (s, 2 H, NCH); $^{13}\text{C NMR}$ δ 17.74 (s, *o*- CH_3), 21.16 (s, *p*- CH_3), 124.32 (s, NCH), 129.65 (s, Mes $\text{C}_{3,5}$), 135.76 (s, Mes $\text{C}_{2,6}$), 136.08 (s, Mes C_1), 139.85 (s, Mes C_4), 175.29 (br s, NCN); $^{15}\text{N NMR}$ (ref $\text{NH}_4^{15}\text{NO}_3$) δ -179.26 ; $^{27}\text{Al NMR}$ (ref $^{27}\text{Al}(\text{H}_2\text{O})_6^{3+}$) δ 107 (br); IR (KBr) 1743 cm^{-1} (br AlH). Anal. Calcd for $\text{C}_{21}\text{H}_{27}\text{N}_3\text{Al}$: C, 75.42; H, 8.14; N, 8.38. Found: C, 75.41; H, 8.08; N, 8.26.

(4) *NMR and the Periodic Table*; Harris, R. K., Mann, B. E., Eds.; Academic Press: New York, 1978; p 279.

(5) For structures of representative imidazolium ions, see: (a) 1,3-Dimethylimidazolium chloride (ref 1, supplementary material). (b) 1,3-Di(1-adamantyl)imidazolium tetraphenylborate (Arduengo, A. J.; Harlow, R. L.; Kline, M. J. *Am. Chem. Soc.* **1991**, *113*, 361; supplementary material). (c) 1,3-Diphenylimidazolium perchlorate (**3**) (Luger, P.; Ruban, G. Z. *Kristallogr.* **1975**, *142*, 177). (d) Langer, V.; Huml, K.; Reck, G. *Acta Crystallogr., Sect. B* **1982**, *38*, 298. (e) Abdul-Sada, A. K.; Greenway, A. M.; Hitchcock, P. B.; Mohammed, T. J.; Seddon, K. R.; Zora, J. A. *J. Chem. Soc., Chem. Commun.* **1986**, 1753.

(6) Crystal data for **2** at -70°C with Mo $\text{K}\alpha$ radiation: $a = 840.9$ (4), $b = 1525.1$ (3), $c = 1645.9$ (8) pm, $\beta = 104.11$ (2) $^\circ$, monoclinic, $P2_1/n$, $Z = 4$, 2065 unique reflections with $I > 3\sigma(I)$. The final R factors were $R = 0.051$ and $R_w = 0.045$. There was a rotational disorder of the three hydrogens on Al that was modeled by two equally populated rotamers. The largest residual electron density in the final difference Fourier map was $0.19\text{ e}/\text{\AA}^3$ near C_2 . Further details of the crystal structure are available in the supplementary material.

(7) This drawing was made with the KANVAS computer graphics program. This program is based on the program SCHAKL of E. Keller (Kristallographisches Institut der Universität Freiburg, Germany), which was modified by A. J. Arduengo, III (E. I. du Pont de Nemours & Co., Wilmington, DE) to produce the back and shadowed planes. The planes bear a 50-pm grid and the lighting source is at infinity so that shadow size is meaningful. Only one rotamer for the disordered AlH_3 group is shown.

(8) Malone, J. F.; McDonald, W. S. *J. Chem. Soc., Dalton Trans.* **1972**, 2646.

Biocatalysis and Nineteenth Century Organic Chemistry: Conversion of D-Glucose into Quinoid Organics

K. M. Draths, T. L. Ward, and J. W. Frost*

Department of Chemistry, Purdue University
West Lafayette, Indiana 47907

Received August 3, 1992

By combining a newly created biocatalyst with nineteenth century chemical methodology,¹ quinoid organics such as quinic